Supplement of The Cryosphere, 17, 2725–2754, 2023
https://doi.org/10.5194/tc-17-2725-2023-supplement

The Cryosphere
Open Access

Supplement of

Post-Little Ice Age rock wall permafrost evolution in Norway

Justyna Czekirda et al.

Correspondence to: Justyna Czekirda (justyna.czekirda@geo.uio.no)

Supplementary Figures

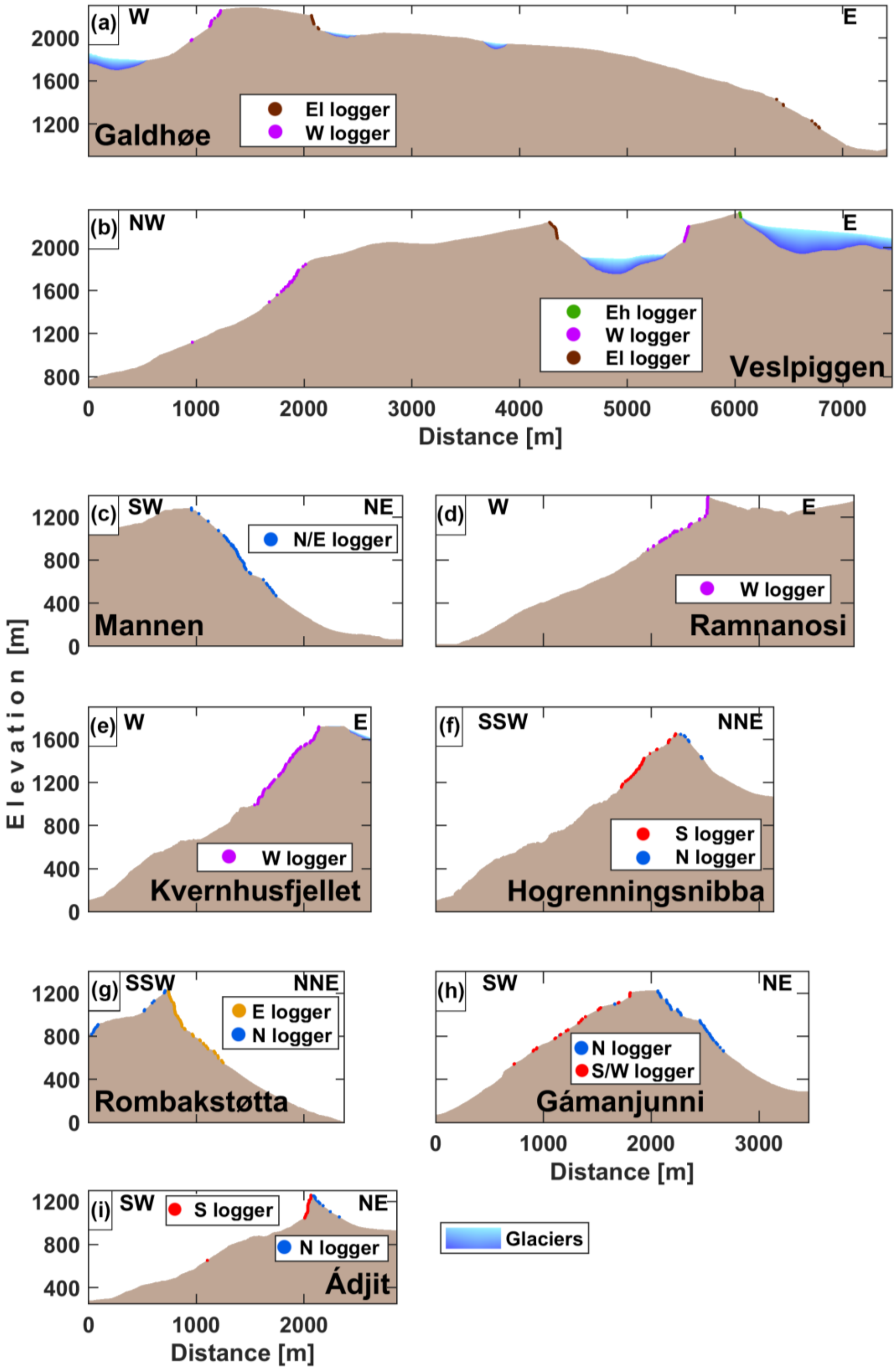

Supplementary Figure S1. Logger data used for the computation of surface offsets arising from the incoming solar shortwave radiation along profiles. E – east-facing logger, N – north-facing logger, S – south-facing logger, W – west-facing logger, suffix "h" – at a higher elevation, suffix "l" – at a lower elevation.

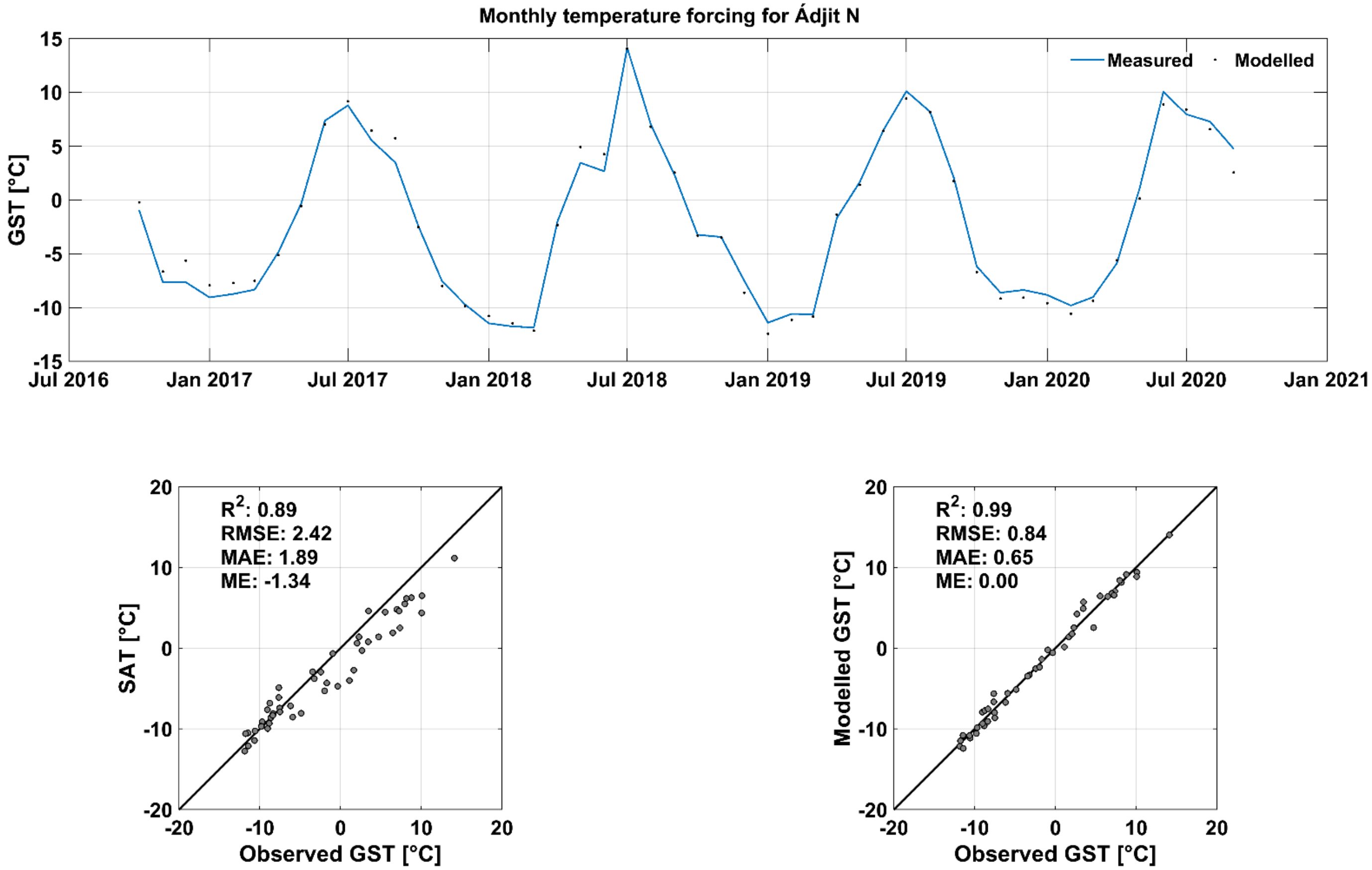

Supplementary Figure S2. Calibration for the north-facing logger at Ádjit. GST-ground surface temperature. SAT-surface air temperature. RMSE-root mean square error. MAE-mean absolute error. ME-mean error.

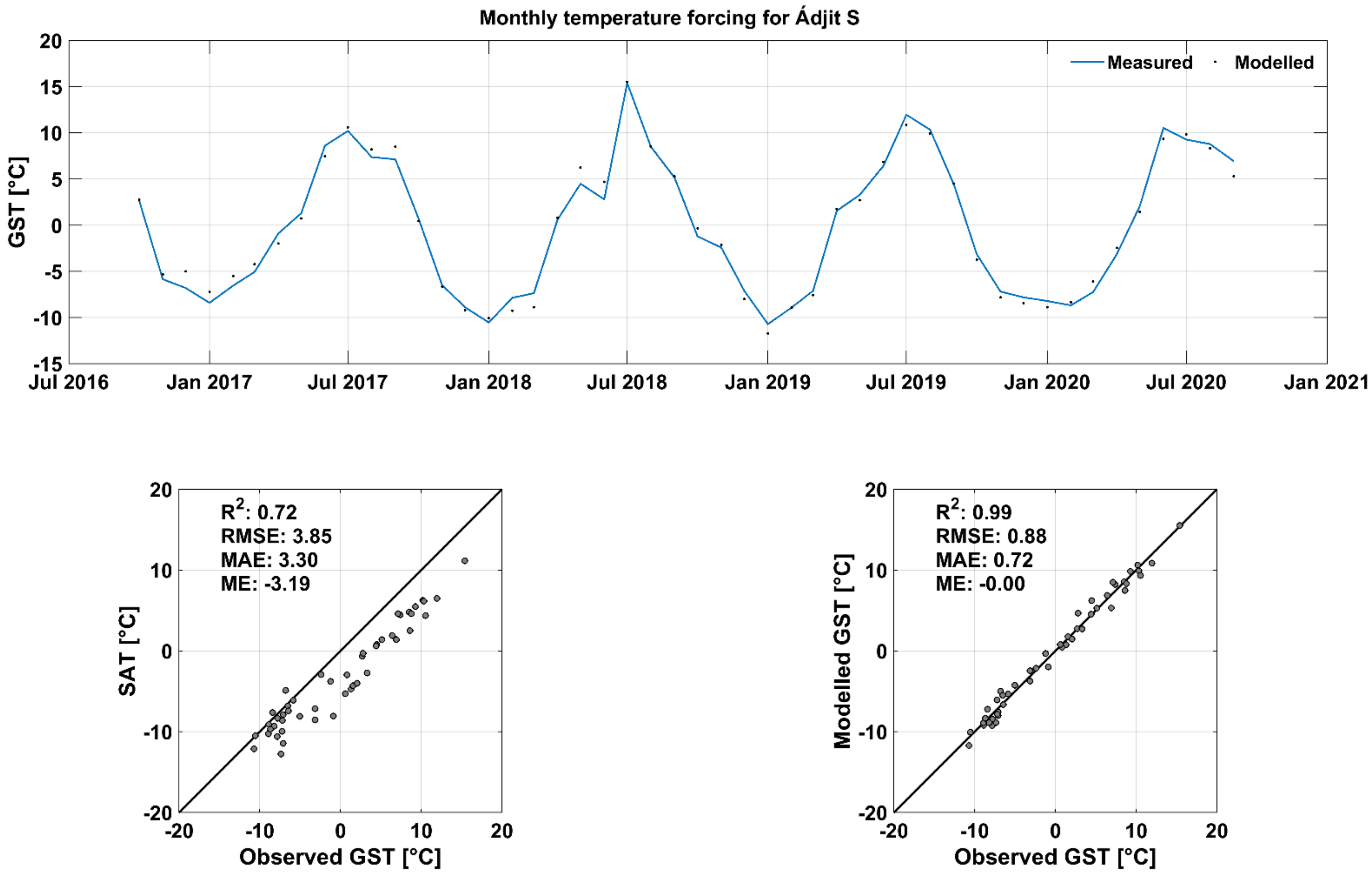

Supplementary Figure S3. Calibration for the higher south-facing logger at Ádjit. GST-ground surface temperature. SAT-surface air temperature. RMSE-root mean square error. MAE-mean absolute error. ME-mean error.

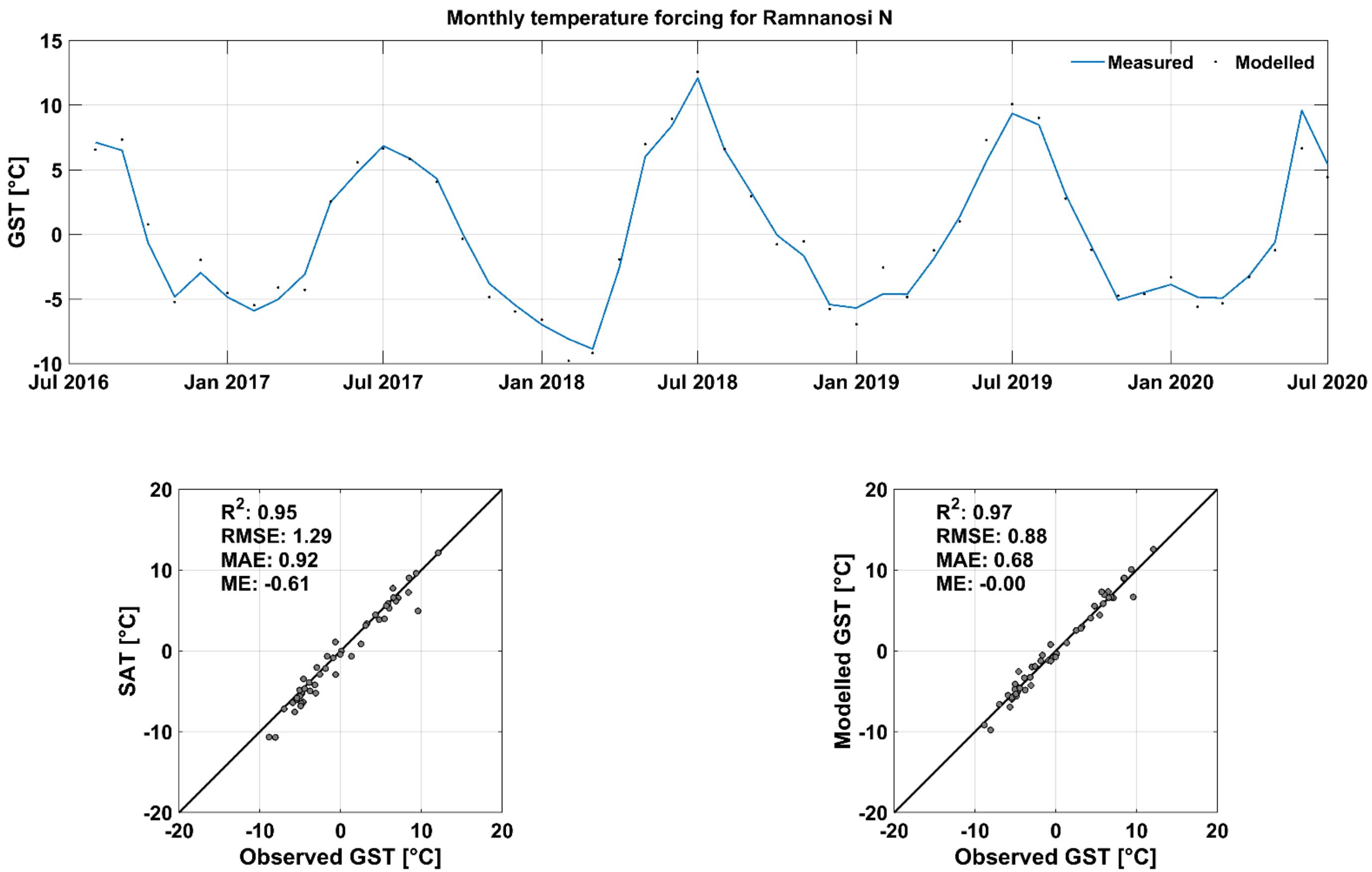

Supplementary Figure S4. Calibration for the north-facing logger at Ramnanosi. GST-ground surface temperature. SAT-surface air temperature. RMSE-root mean square error. MAE-mean absolute error. ME-mean error.

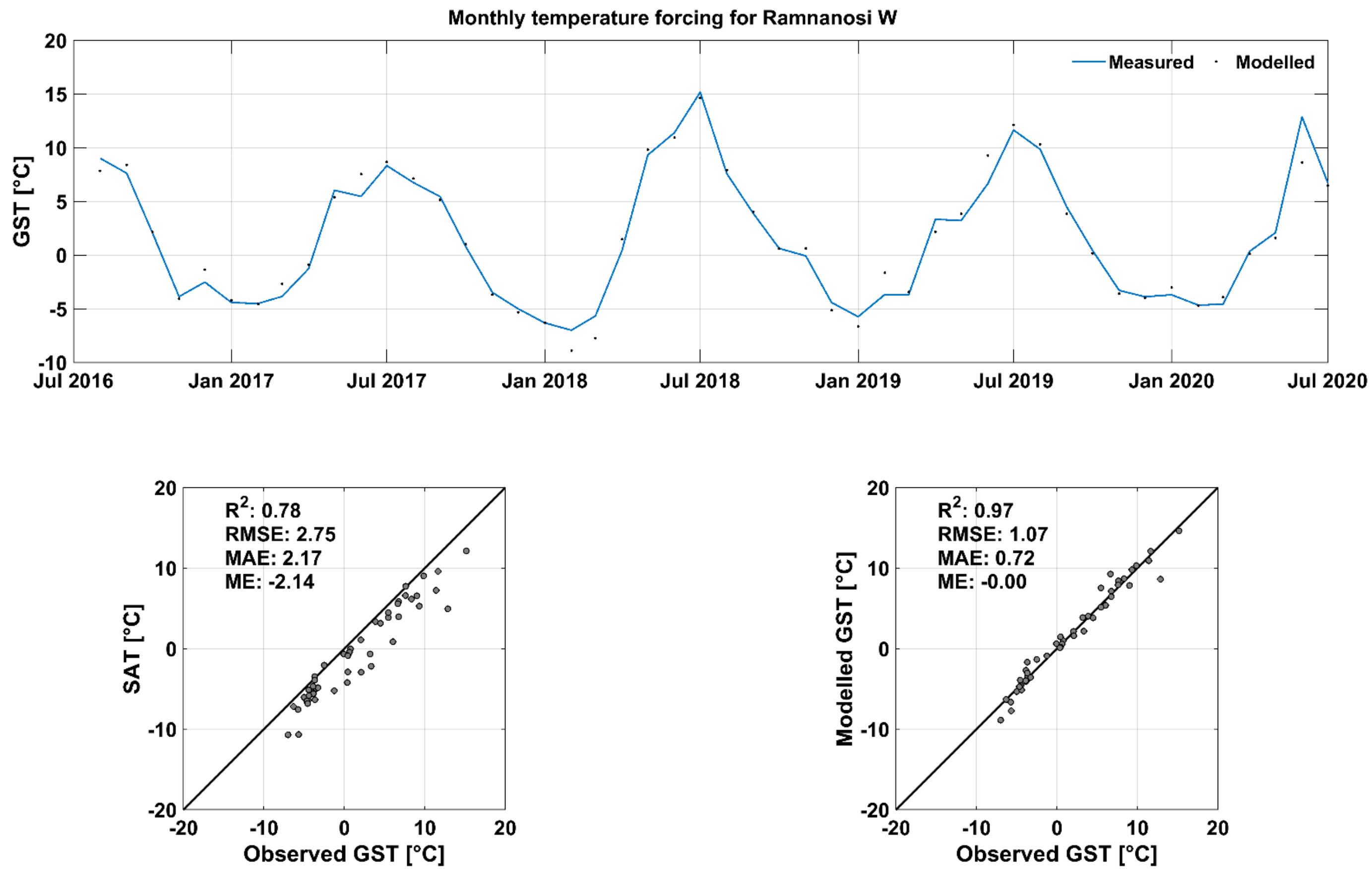

Supplementary Figure S5. Calibration for the west-facing logger at Ramnanosi. GST-ground surface temperature. SAT-surface air temperature. RMSE-root mean square error. MAE-mean absolute error. ME-mean error.

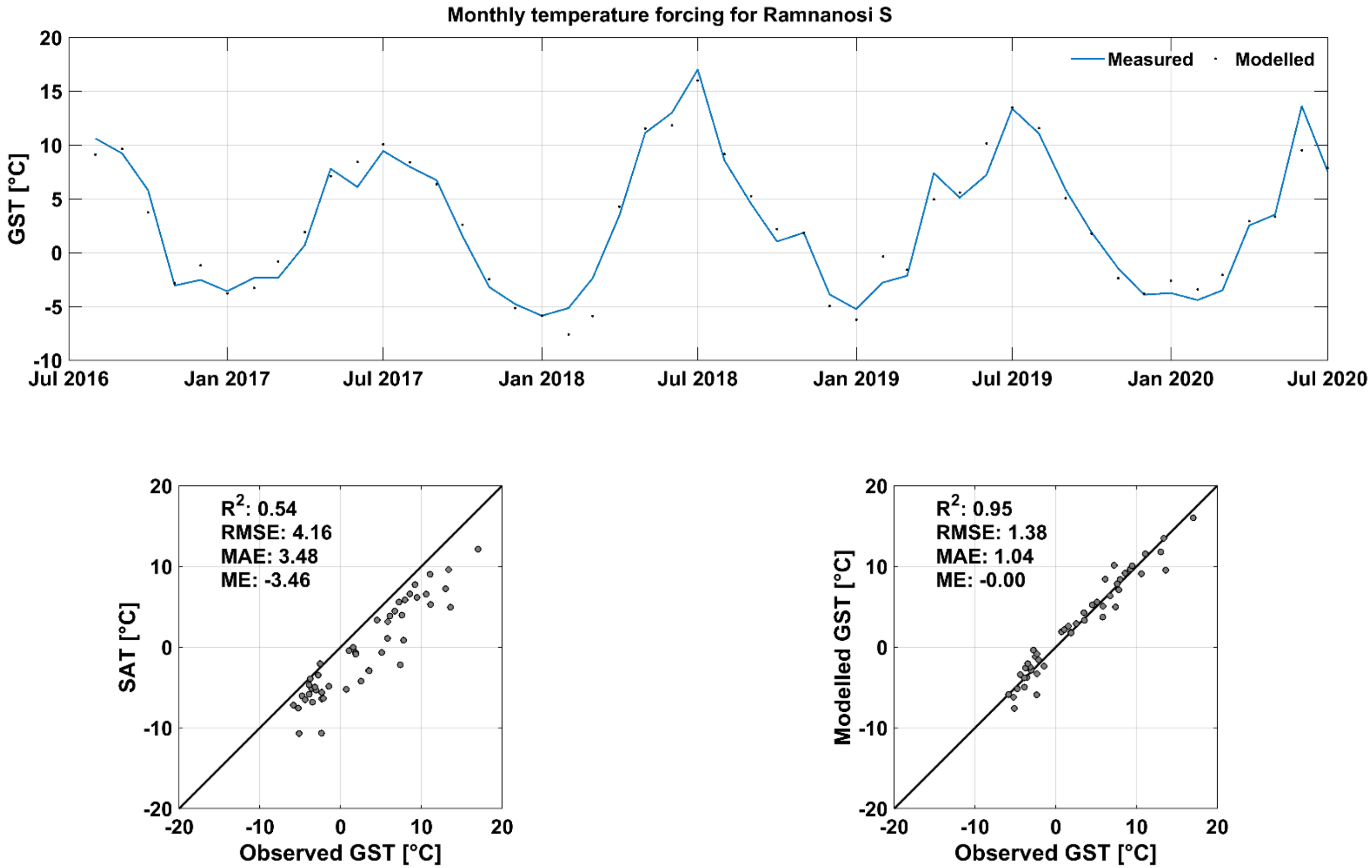

Supplementary Figure S6. Calibration for the south-facing logger at Ramnanosi. GST-ground surface temperature. SAT-surface air temperature. RMSE-root mean square error. MAE-mean absolute error. ME-mean error.

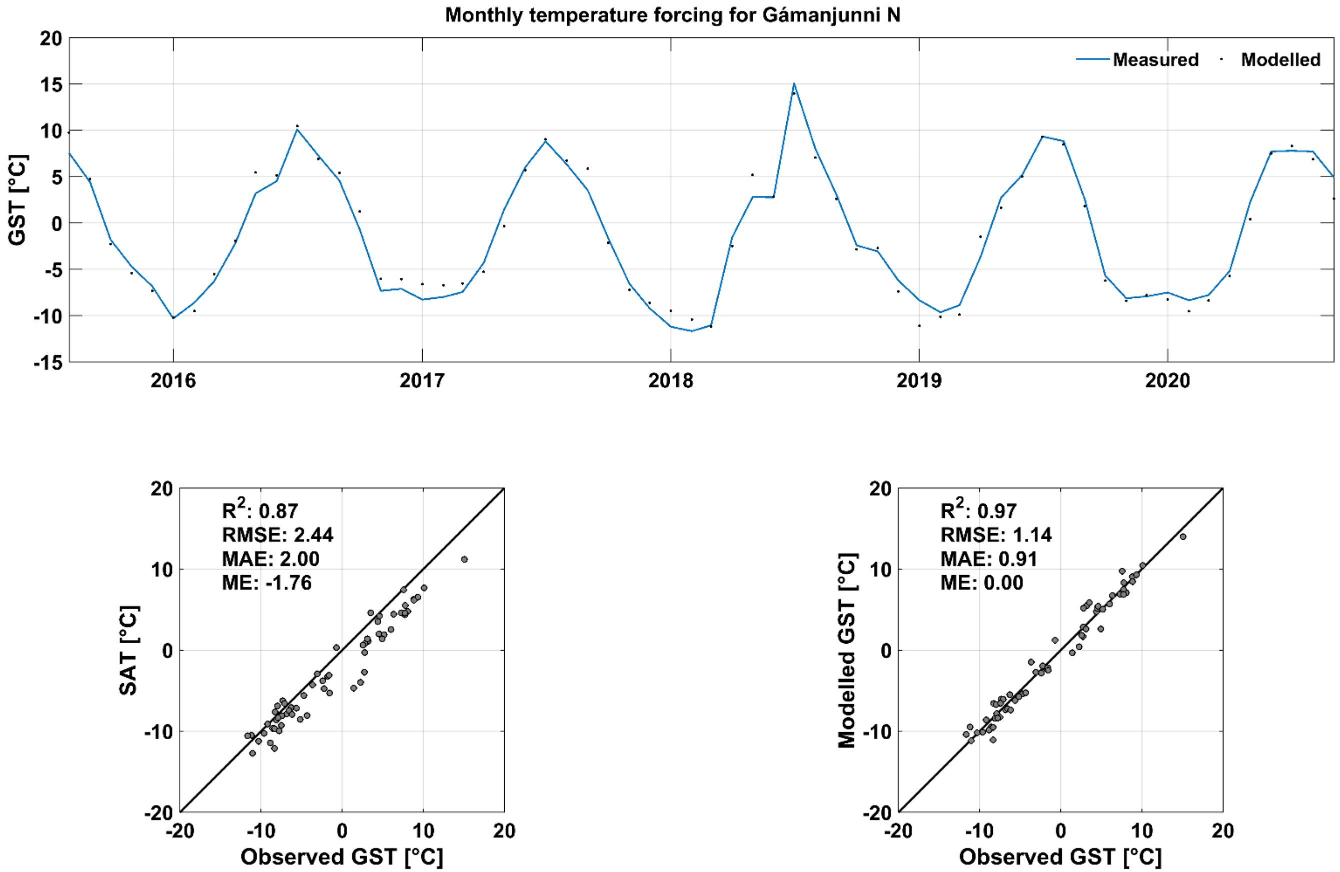

Supplementary Figure S7. Calibration for the north-facing logger at Gámanjunni. GST-ground surface temperature. SAT-surface air temperature. RMSE-root mean square error. MAE-mean absolute error. ME-mean error.

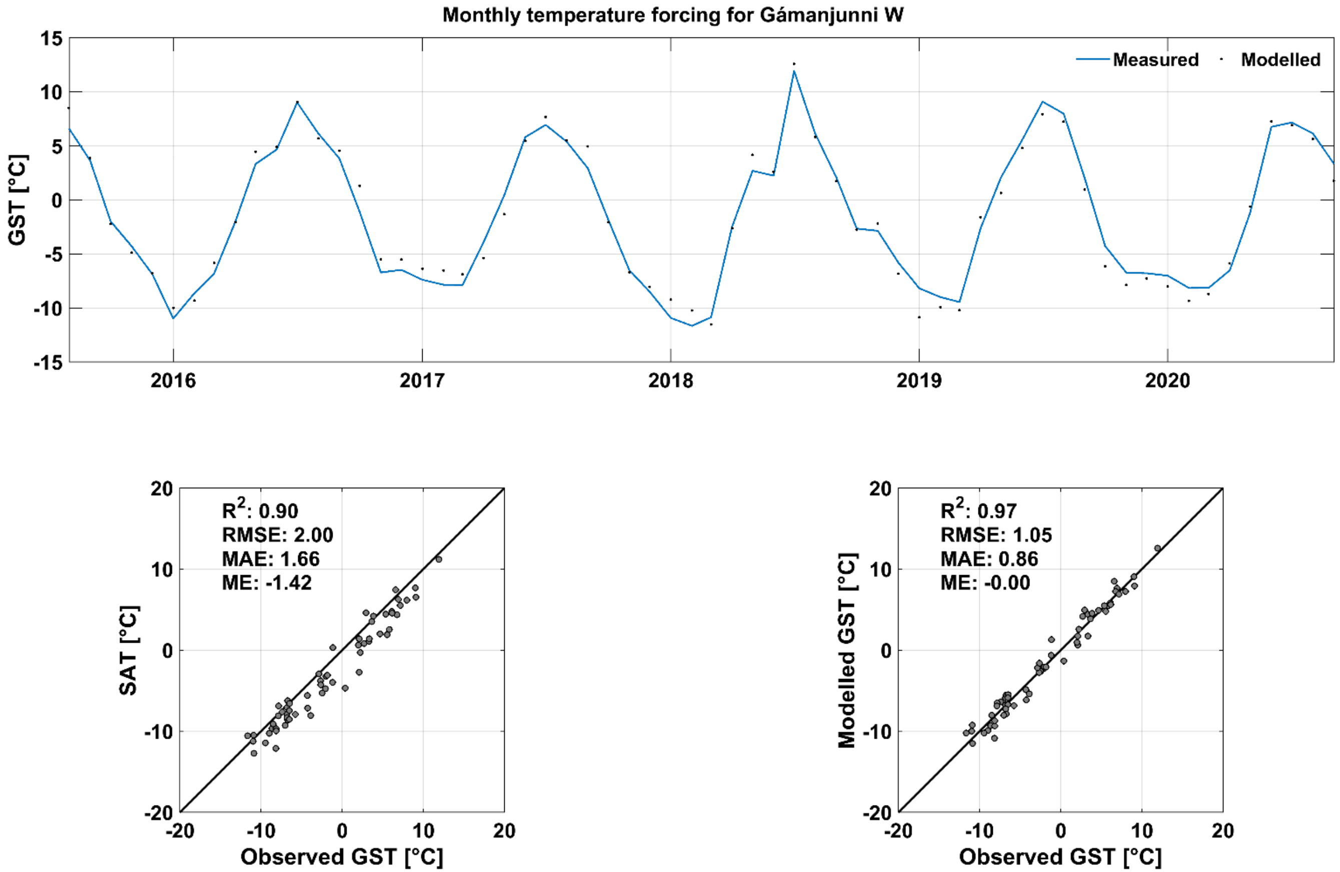

Supplementary Figure S8. Calibration for the west-facing logger at Gámanjunni. GST-ground surface temperature. SAT-surface air temperature. RMSE-root mean square error. MAE-mean absolute error. ME-mean error.

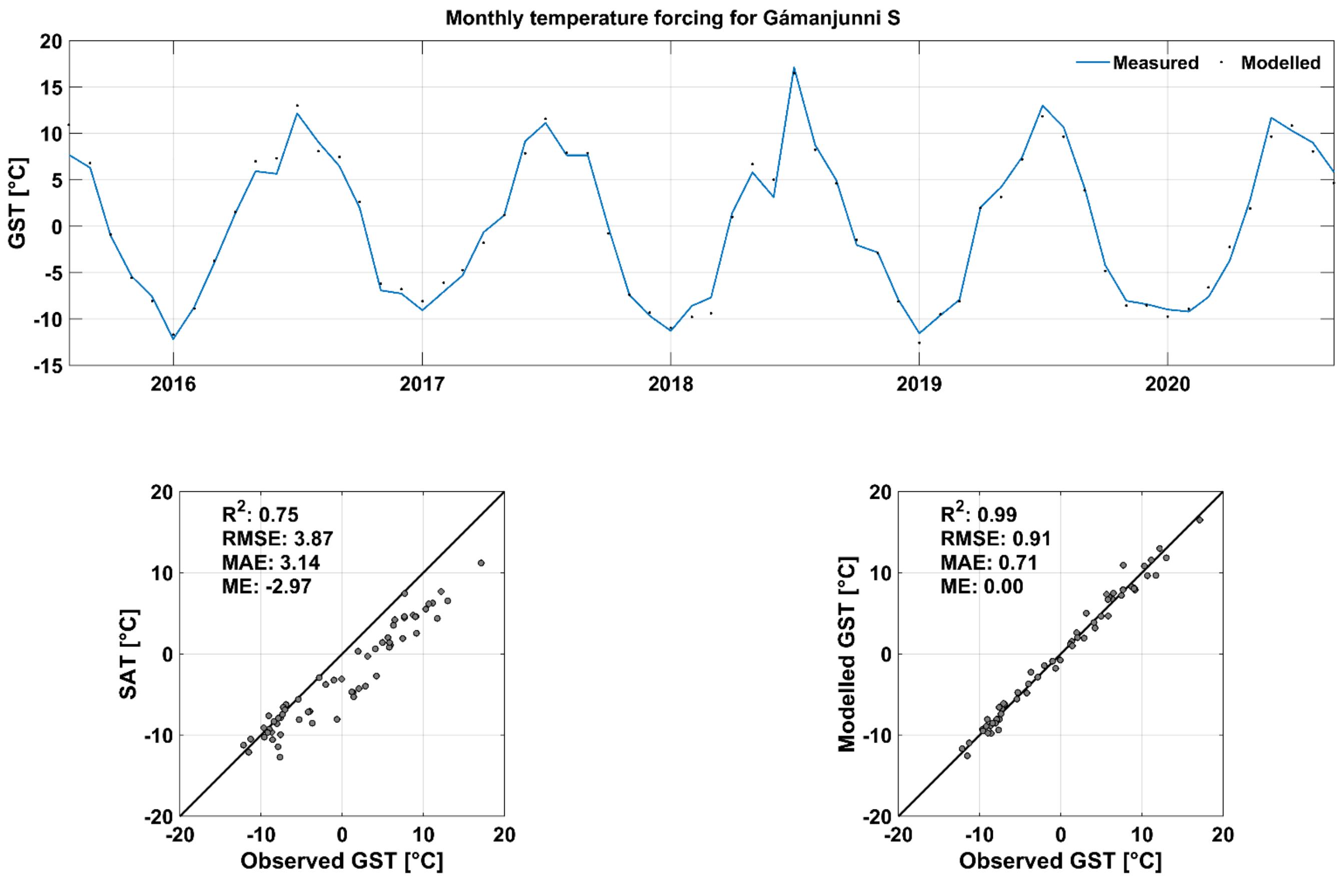

Supplementary Figure S9. Calibration for the south-facing logger at Gámanjunni. GST-ground surface temperature. SAT-surface air temperature. RMSE-root mean square error. MAE-mean absolute error. ME-mean error.

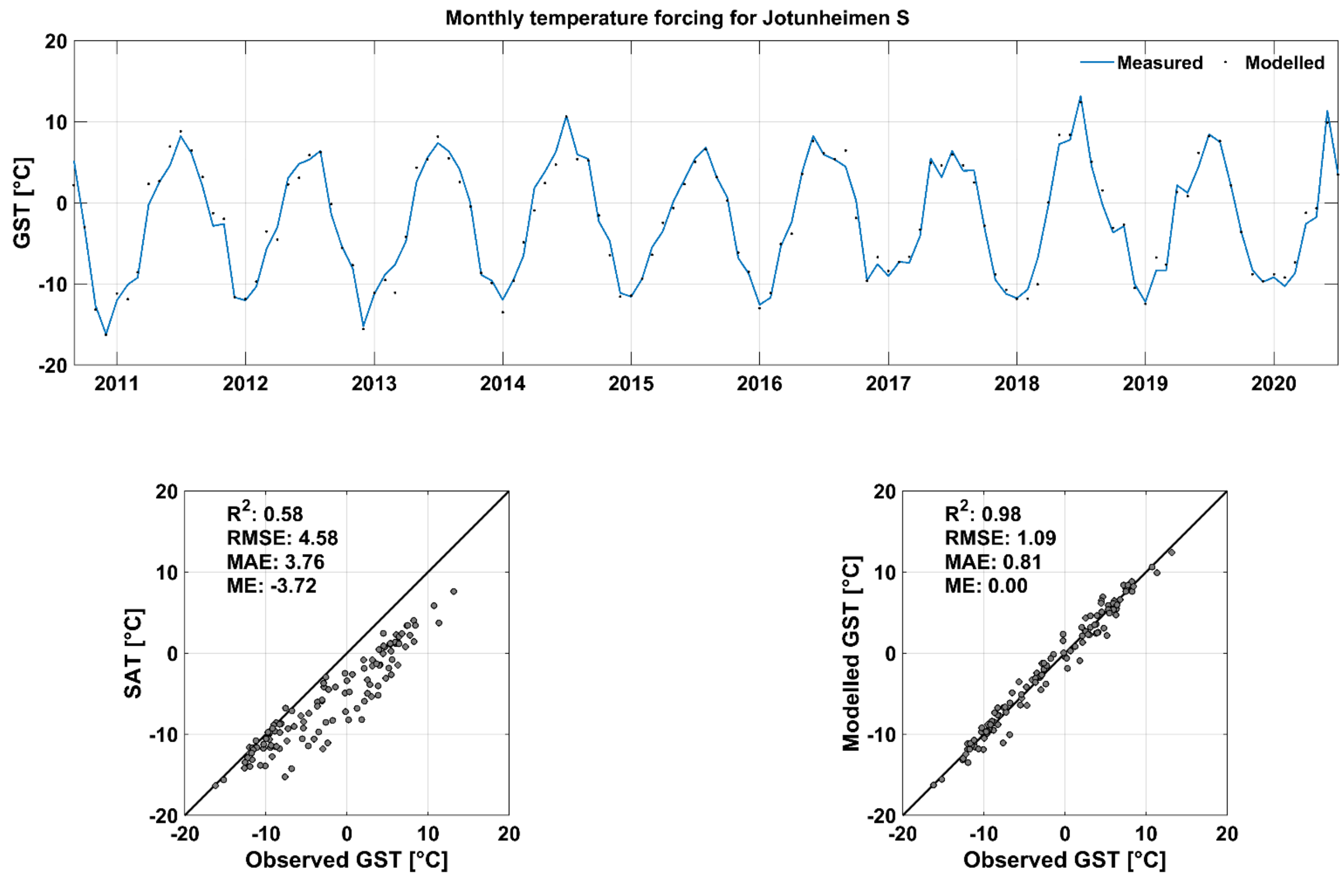

Supplementary Figure S10. Calibration for the south-facing logger at Jotunheimen. GST-ground surface temperature. SAT-surface air temperature. RMSE-root mean square error. MAE-mean absolute error. ME-mean error.

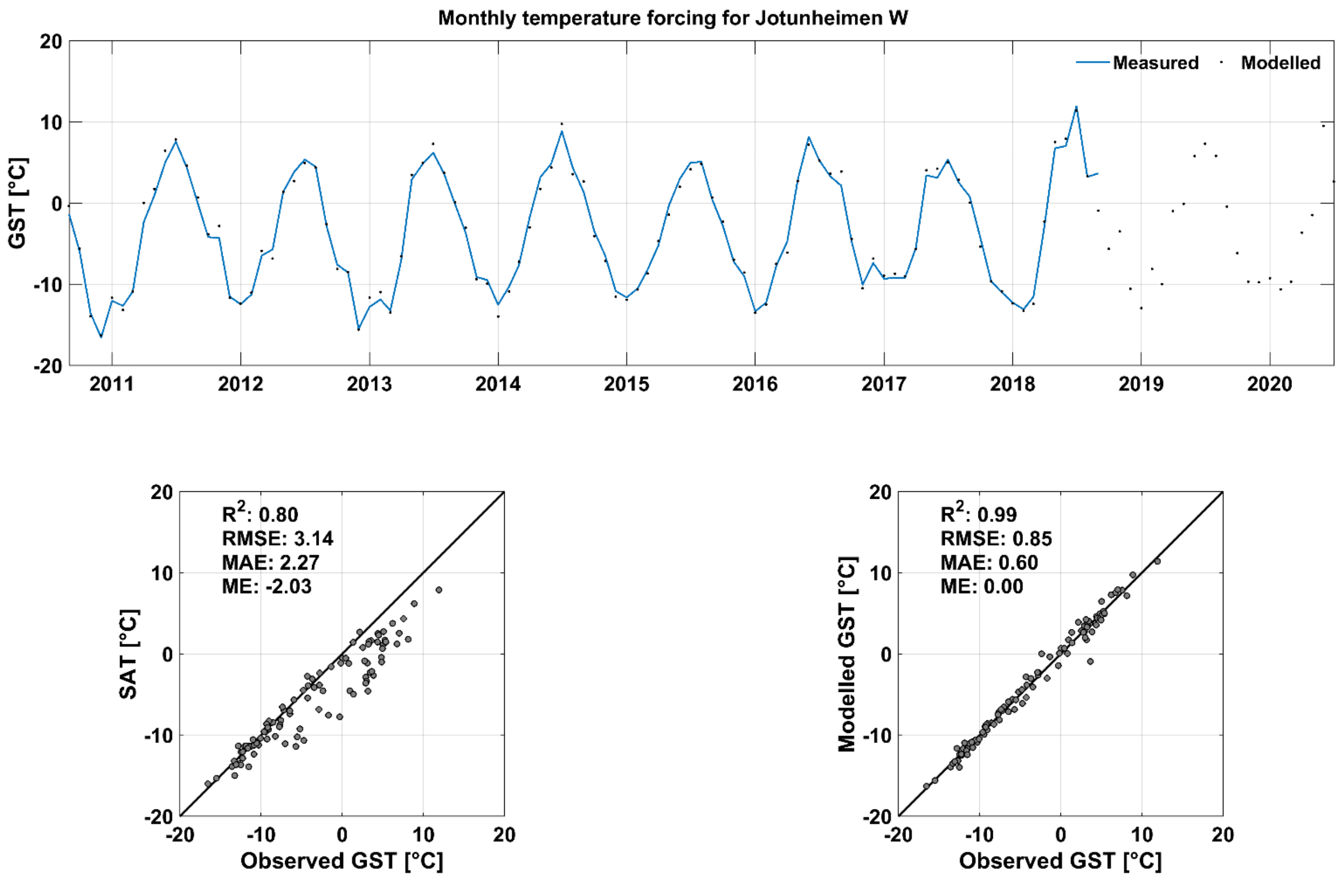

Supplementary Figure S11. Calibration for the west-facing logger at Jotunheimen. GST-ground surface temperature. SAT-surface air temperature. RMSE-root mean square error. MAE-mean absolute error. ME-mean error.

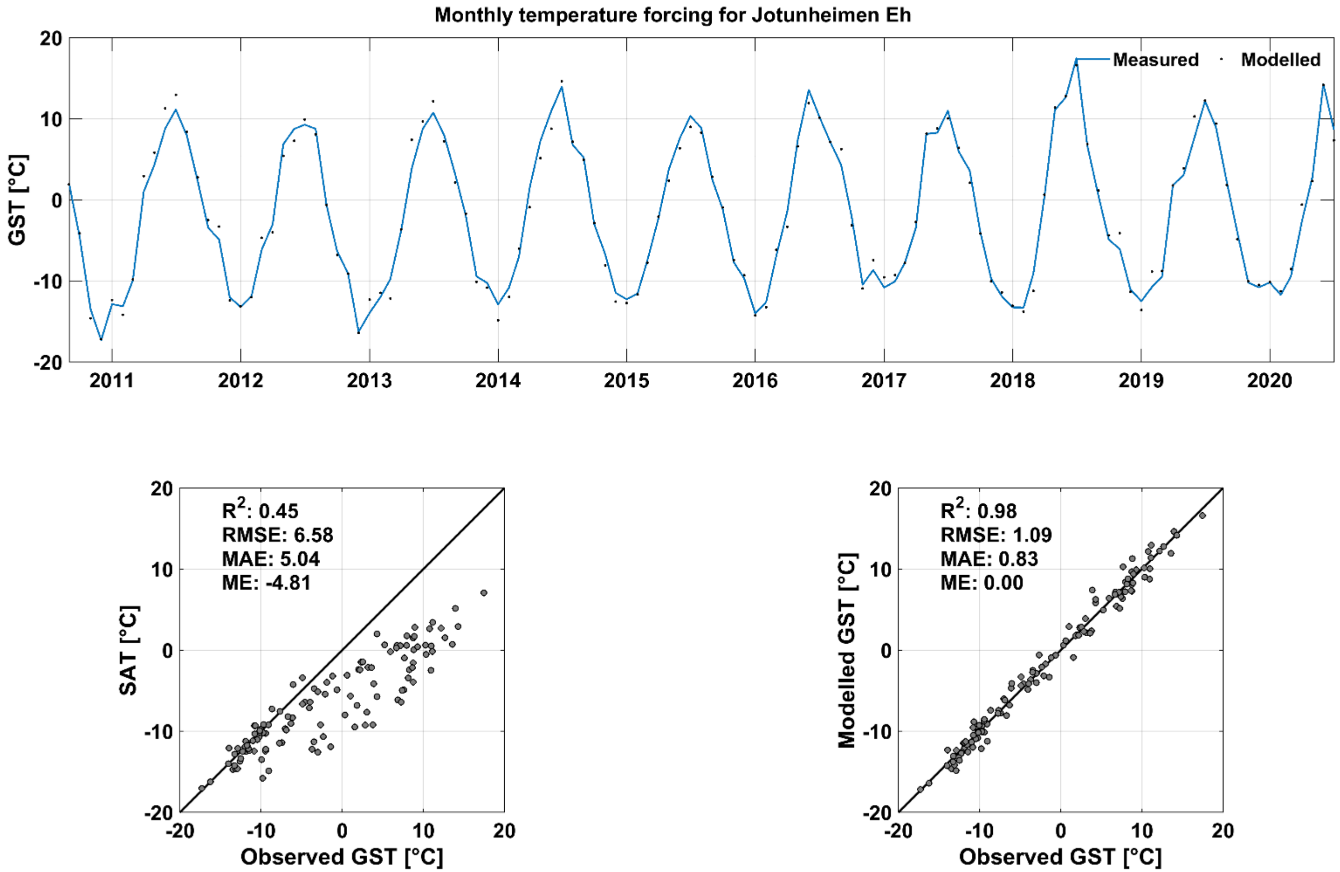

Supplementary Figure S12. Calibration for the higher east-facing logger at Jotunheimen. GST-ground surface temperature. SAT-surface air temperature. RMSE-root mean square error. MAE-mean absolute error. ME-mean error.

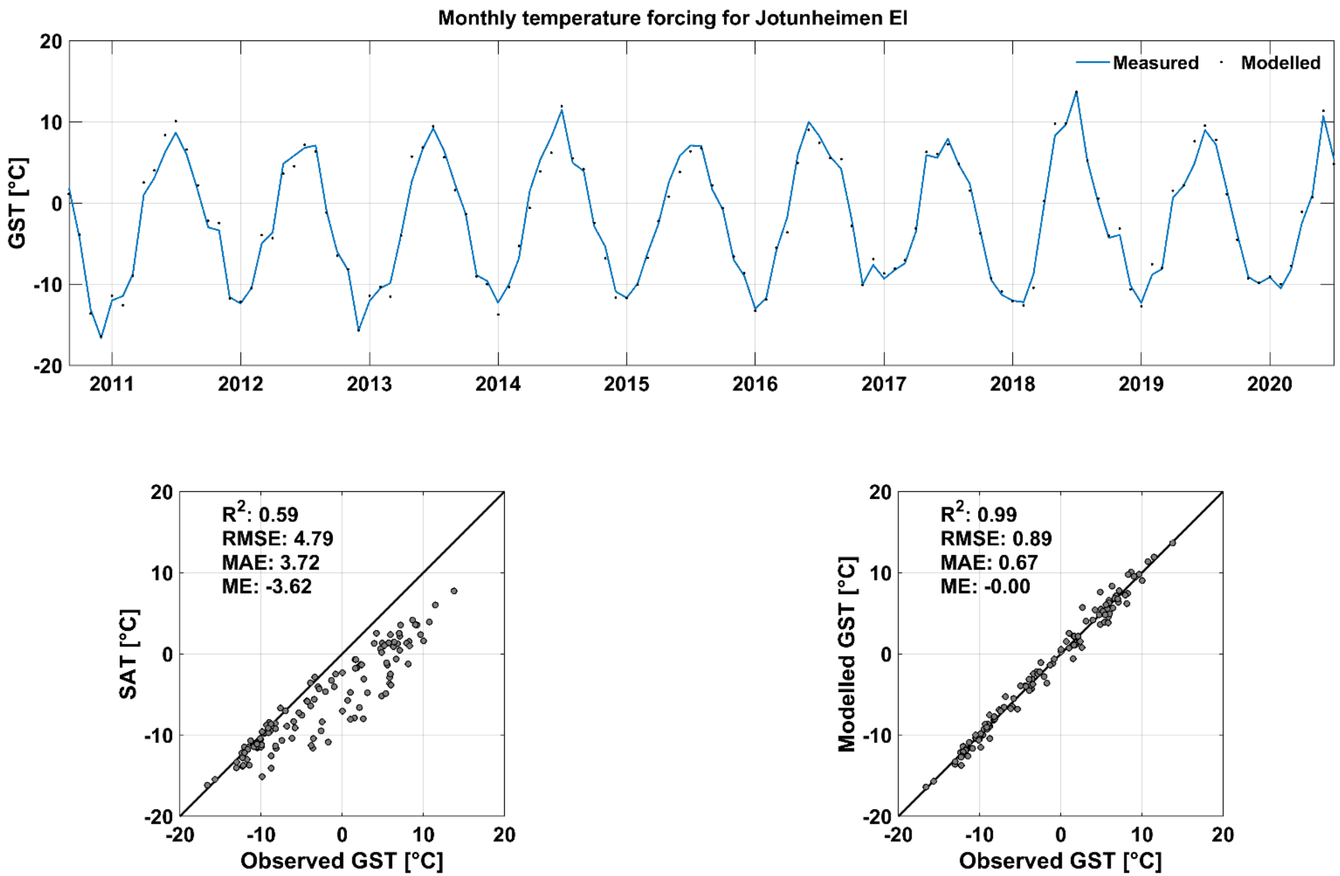

Supplementary Figure S13. Calibration for the lower east-facing logger at Jotunheimen. GST-ground surface temperature. SAT-surface air temperature. RMSE-root mean square error. MAE-mean absolute error. ME-mean error.

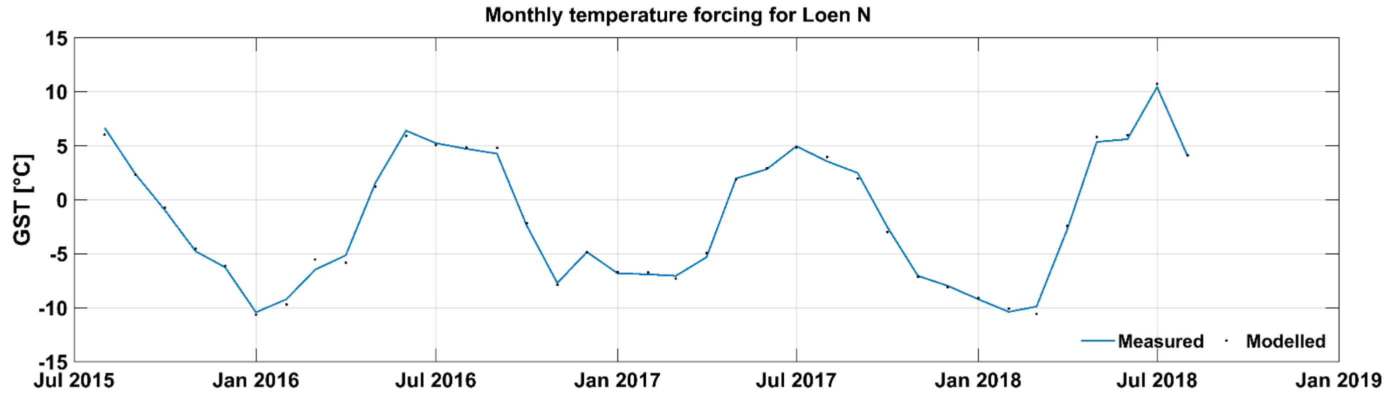

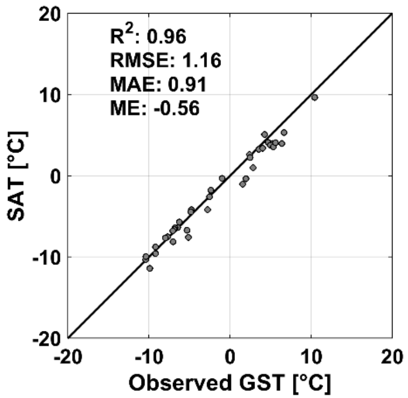

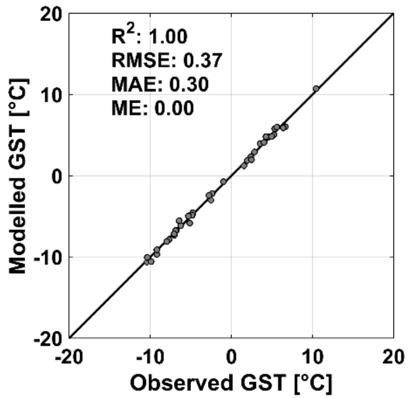

Supplementary Figure S14. Calibration for the north-facing logger at Loen. GST-ground surface temperature. SAT-surface air temperature. RMSE-root mean square error. MAE-mean absolute error. ME-mean error.

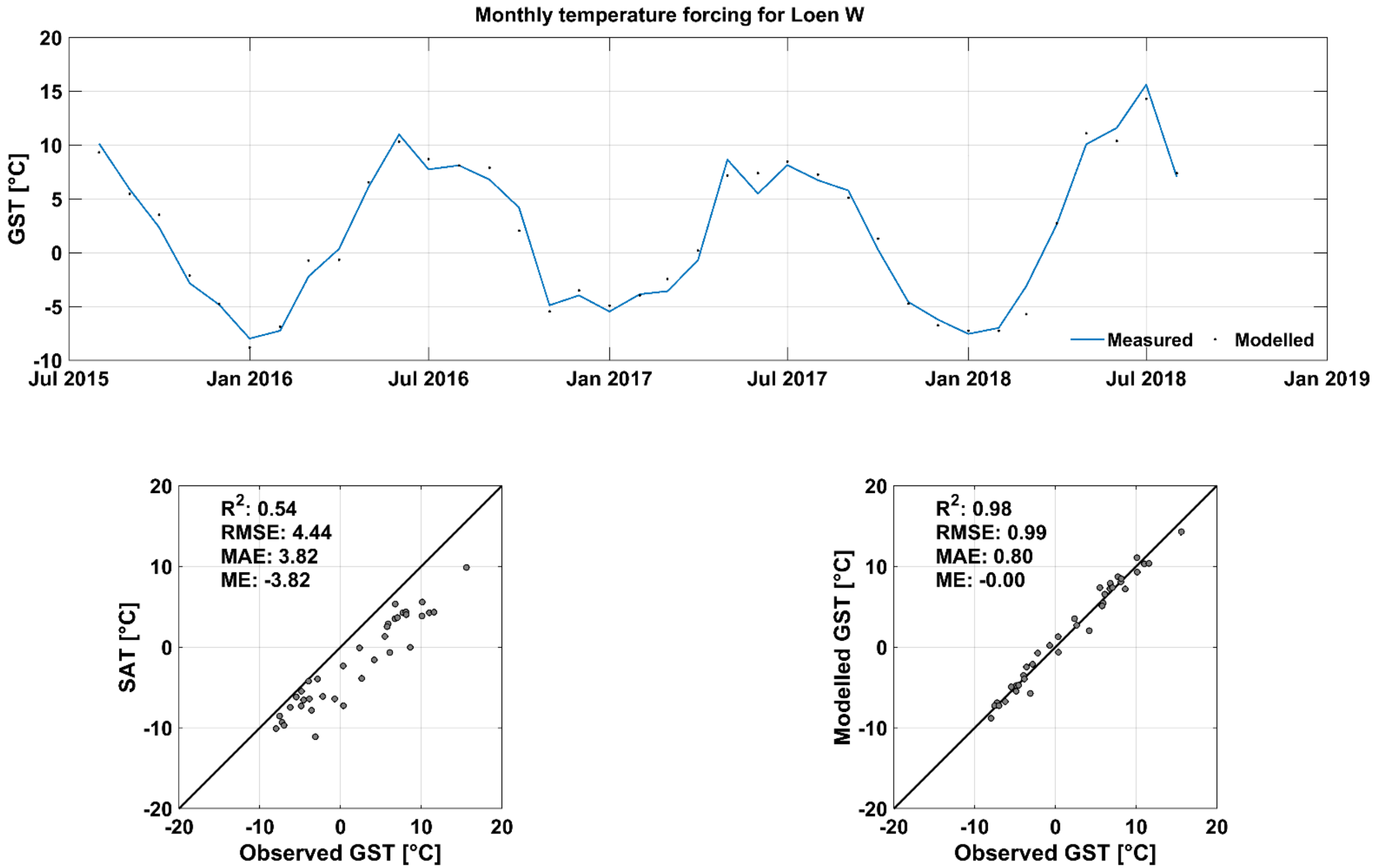

Supplementary Figure S15. Calibration for the west-facing logger at Loen. GST-ground surface temperature. SAT-surface air temperature. RMSE-root mean square error. MAE-mean absolute error. ME-mean error.

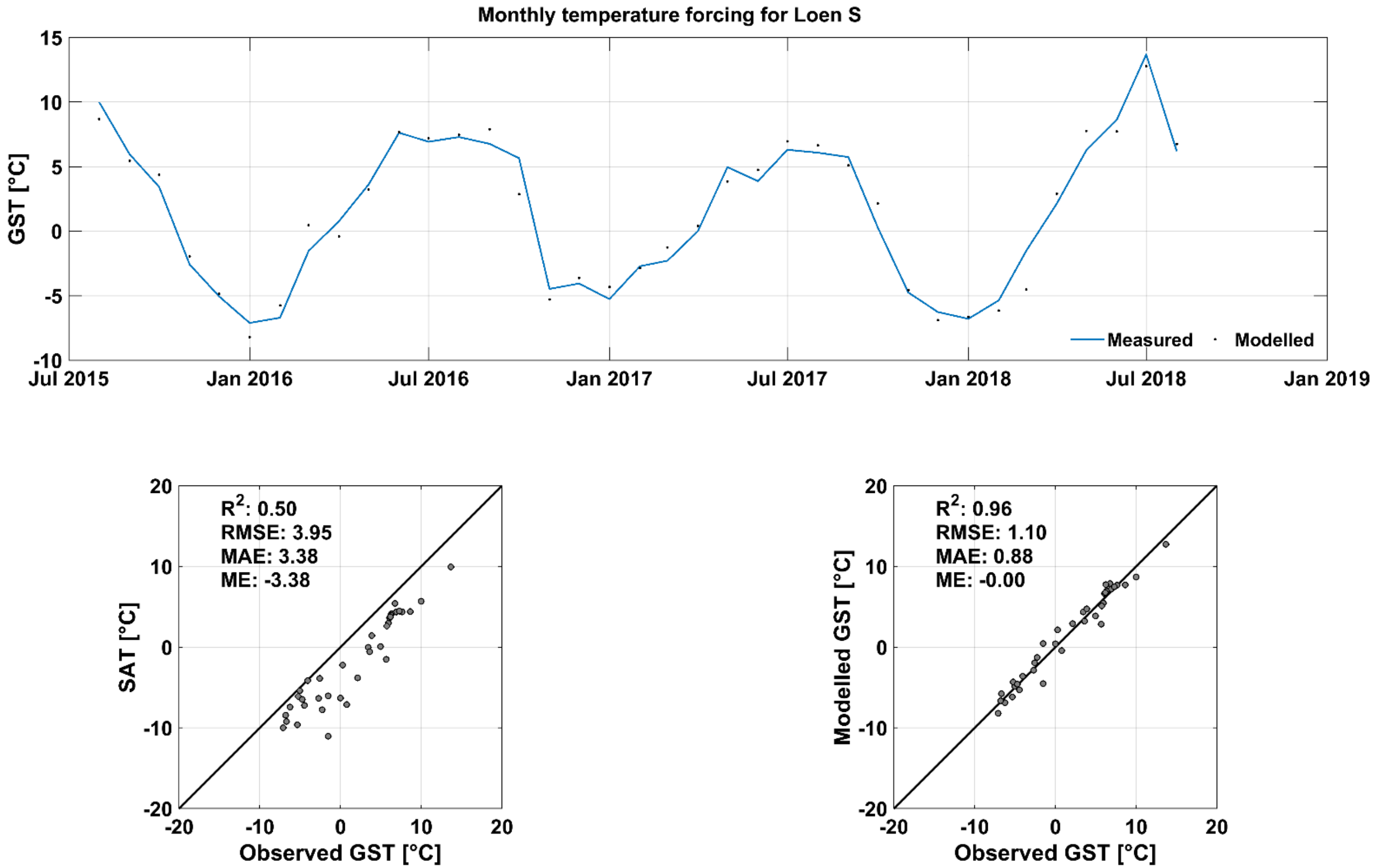

Supplementary Figure S16. Calibration for the south-facing logger at Loen. GST-ground surface temperature. SAT-surface air temperature. RMSE-root mean square error. MAE-mean absolute error. ME-mean error.

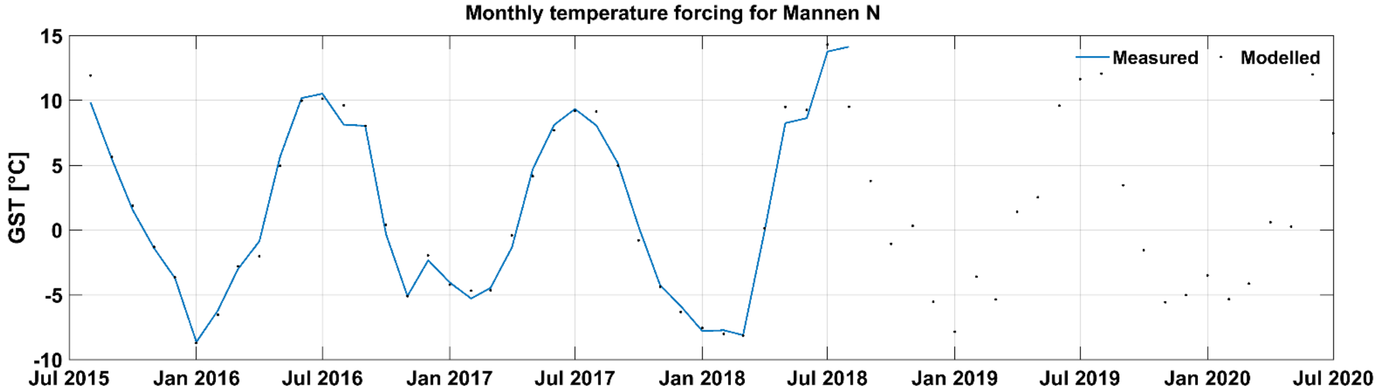

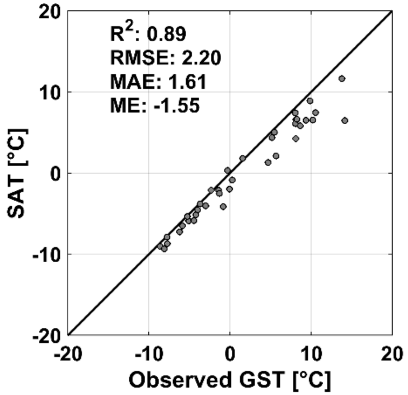

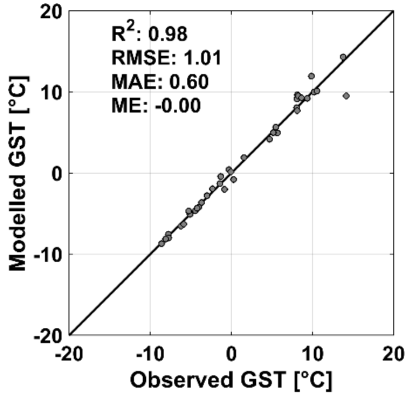

Supplementary Figure S17. Calibration for the north-facing logger at Mannen. GST-ground surface temperature. SAT-surface air temperature. RMSE-root mean square error. MAE-mean absolute error. ME-mean error.

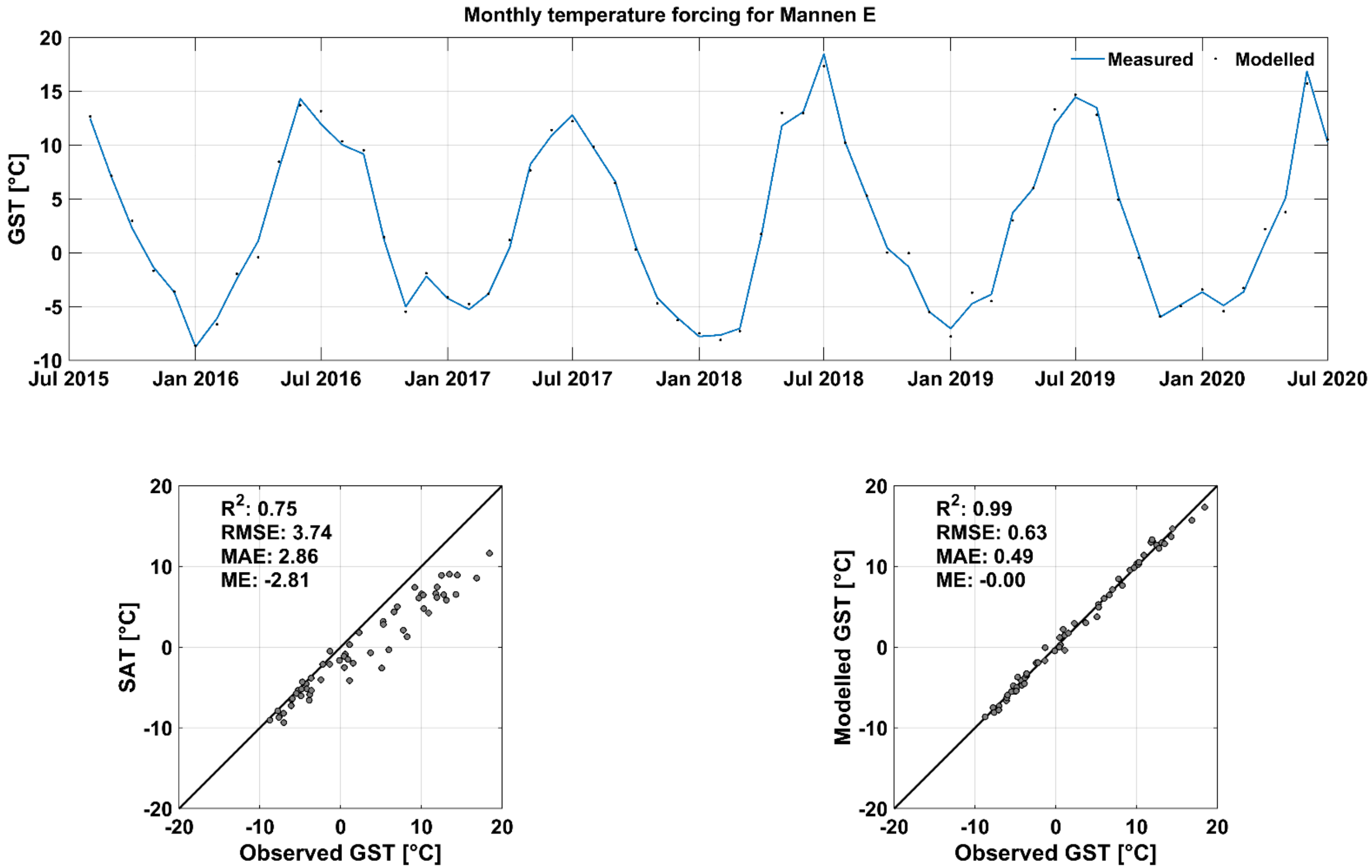

Supplementary Figure S18. Calibration for the east-facing logger at Mannen. GST-ground surface temperature. SAT-surface air temperature. RMSE-root mean square error. MAE-mean absolute error. ME-mean error.

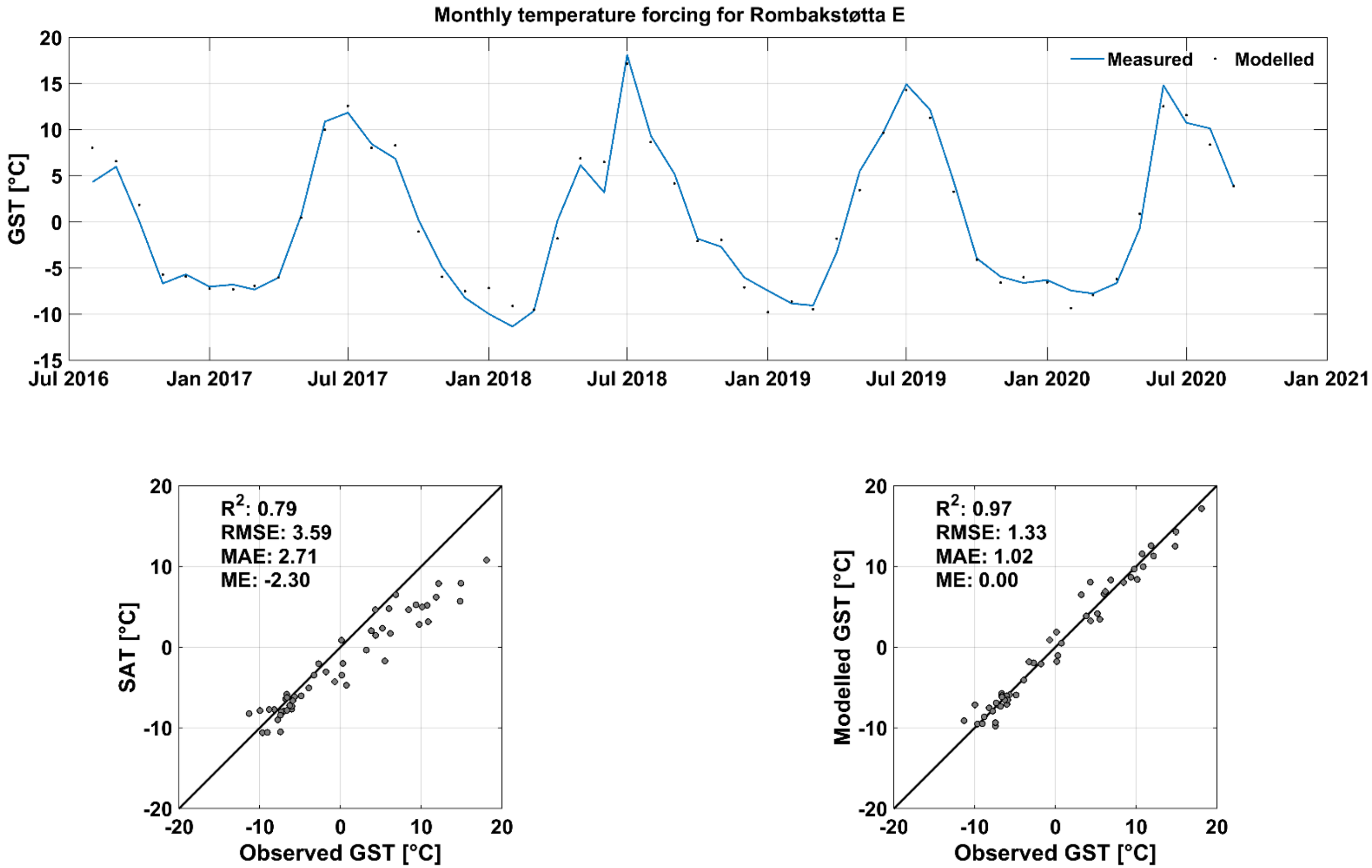

Supplementary Figure S19. Calibration for the east-facing logger at Rombakstøtta. GST-ground surface temperature. SAT-surface air temperature. RMSE-root mean square error. MAE-mean absolute error. ME-mean error.

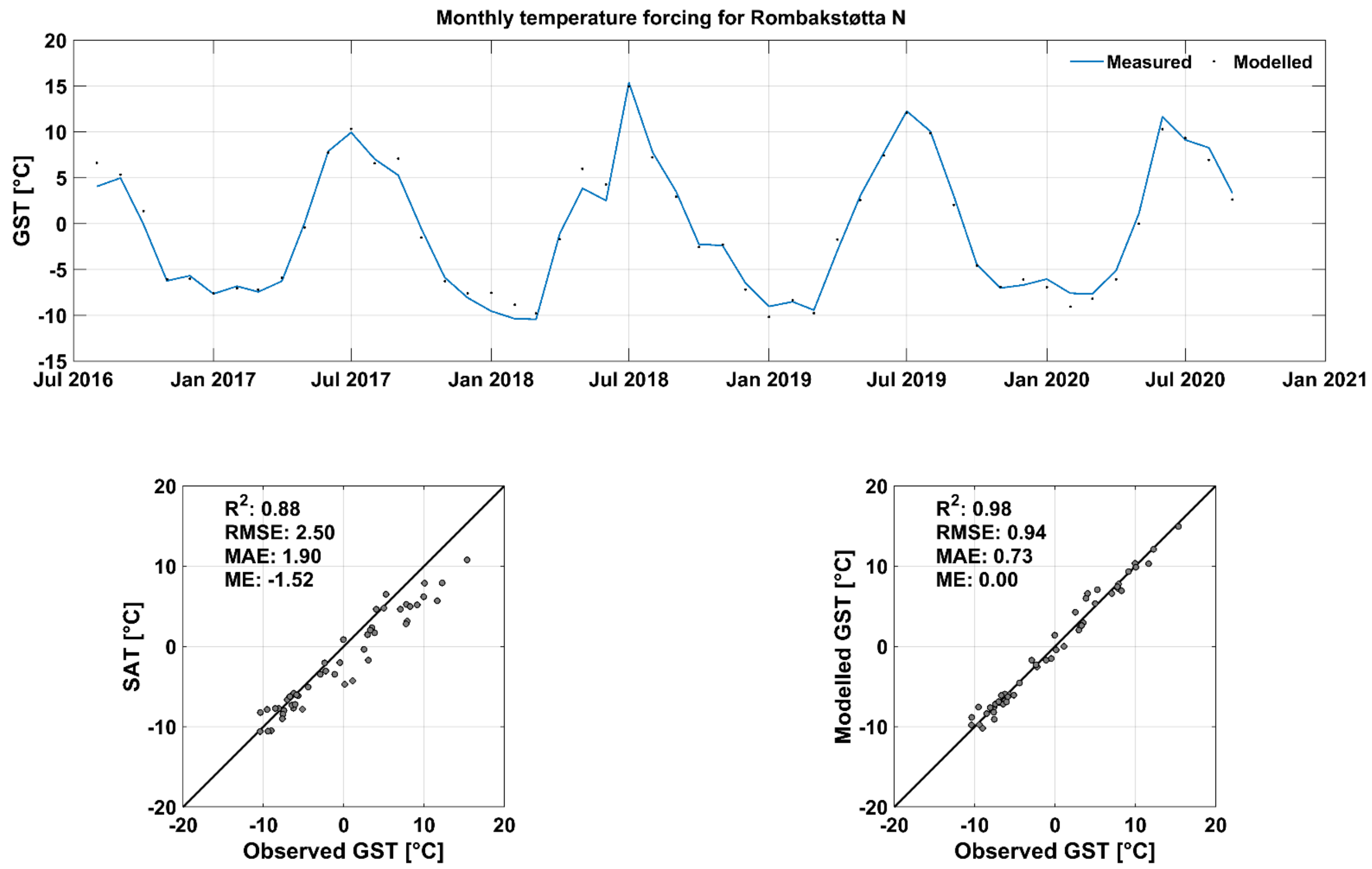

Supplementary Figure S20. Calibration for the north-facing logger at Rombakstøtta. GST-ground surface temperature. SAT-surface air temperature. RMSE-root mean square error. MAE-mean absolute error. ME-mean error.

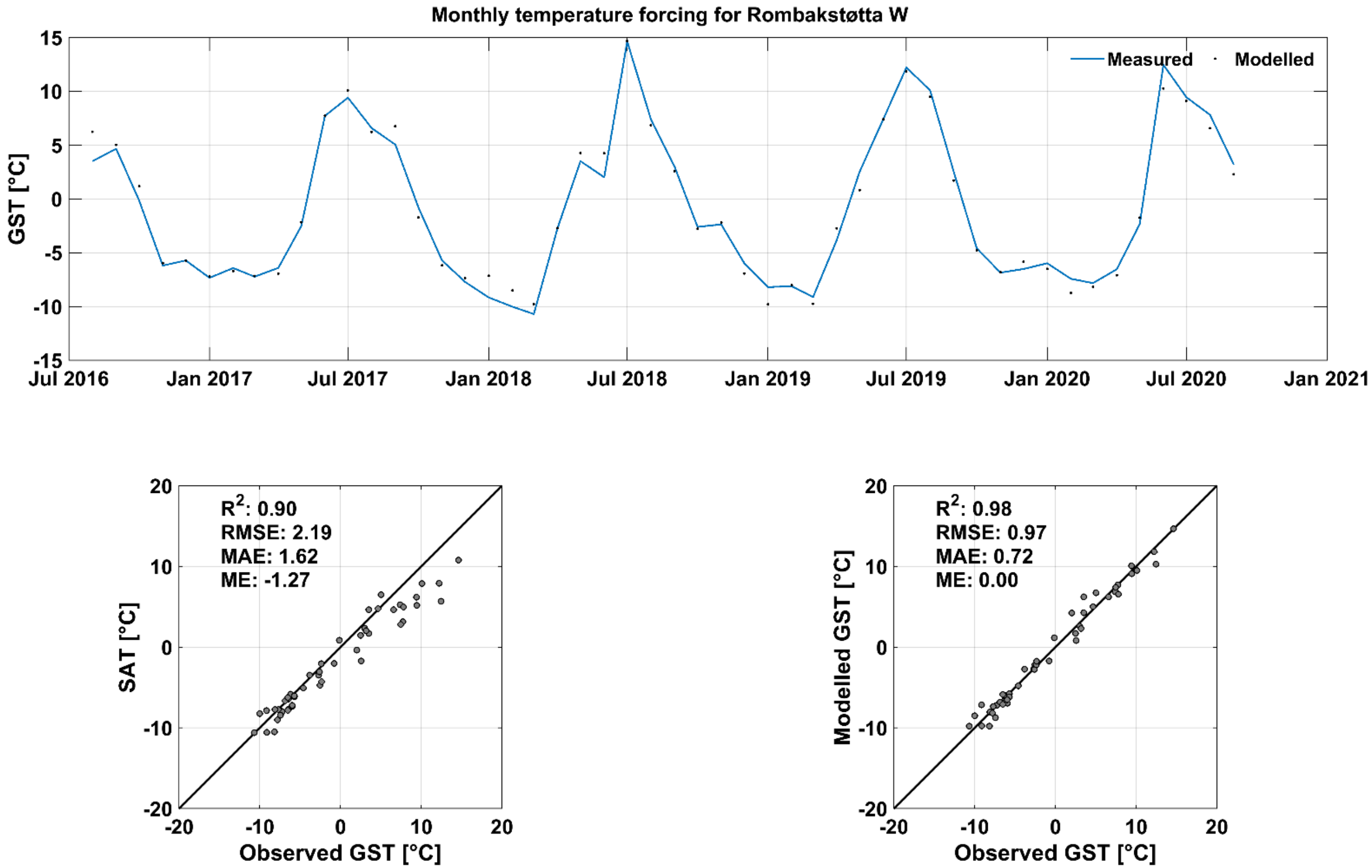

Supplementary Figure S21. Calibration for the west-facing logger at Rombakstøtta. GST-ground surface temperature. SAT-surface air temperature. RMSE-root mean square error. MAE-mean absolute error. ME-mean error.

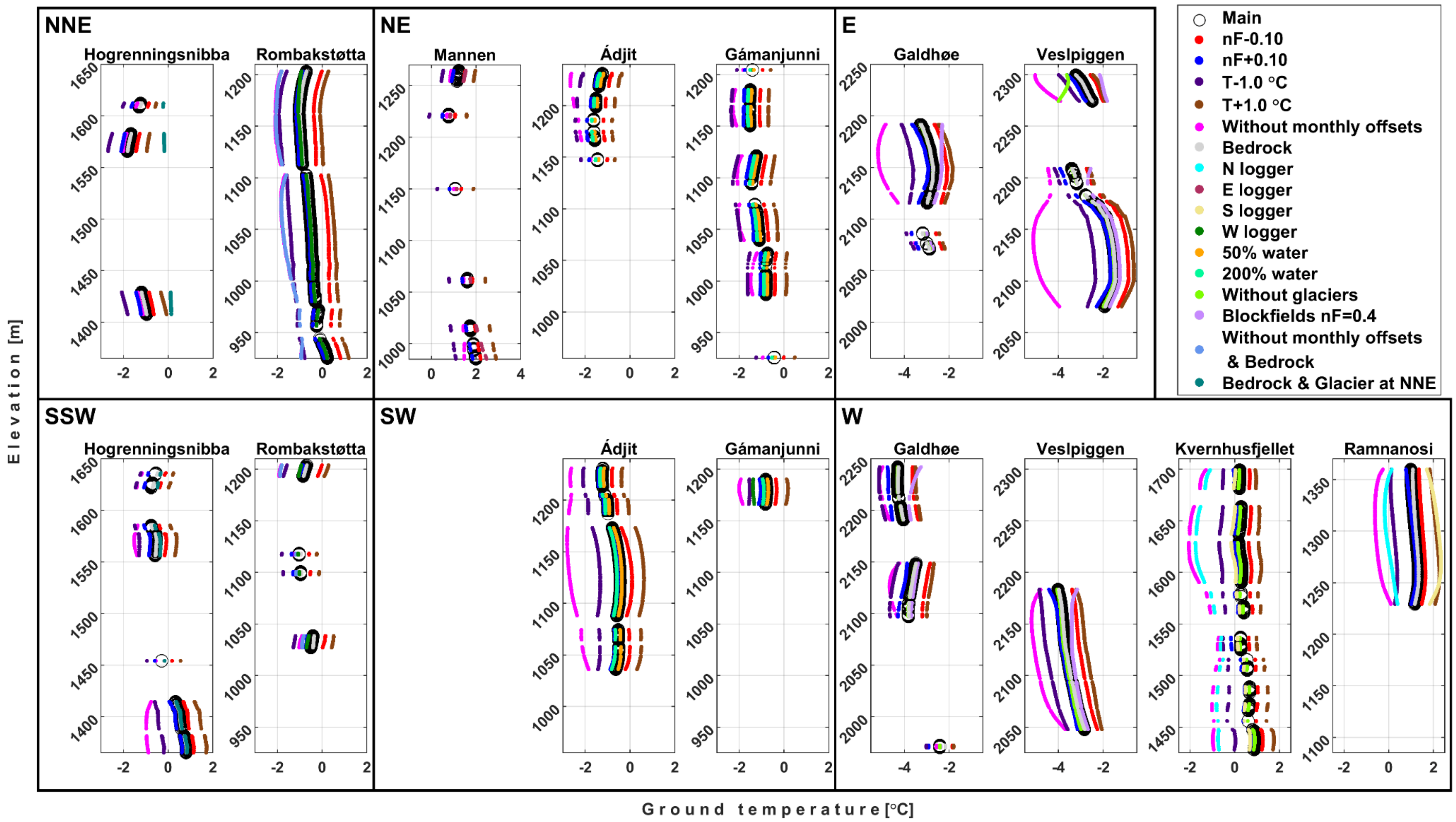

Supplementary Figure S22. Ground temperature in rock walls at 20 m depth for various simulations over the 2010s. A cluster of values without any break elevation-wise usually represents a single rock wall.

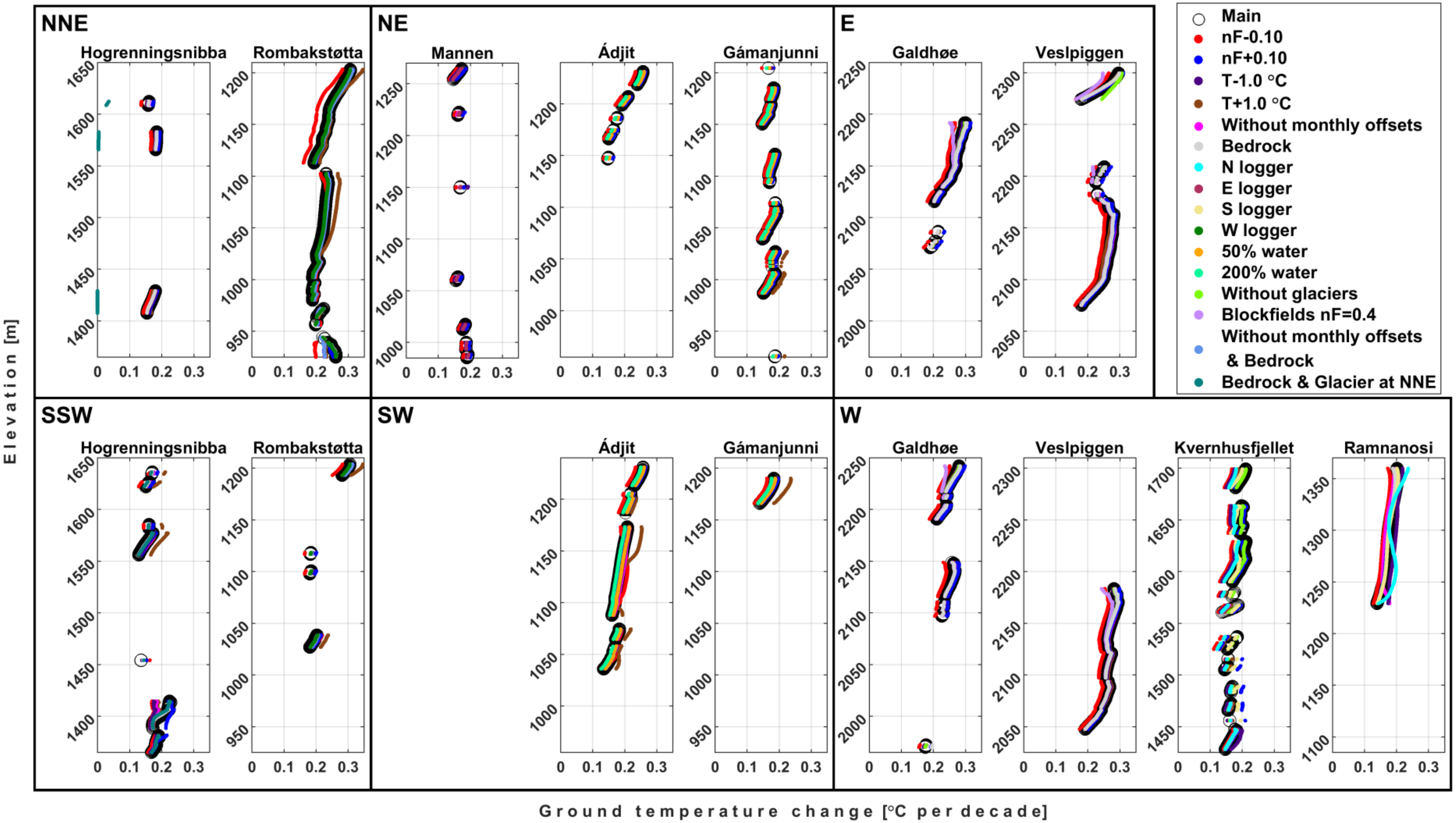

Supplementary Figure S23. Rates of ground temperature change in rock walls at 20 m depth for various simulations between the 1980s and 2010s. A cluster of values without any break elevation-wise usually represents a single rock wall.

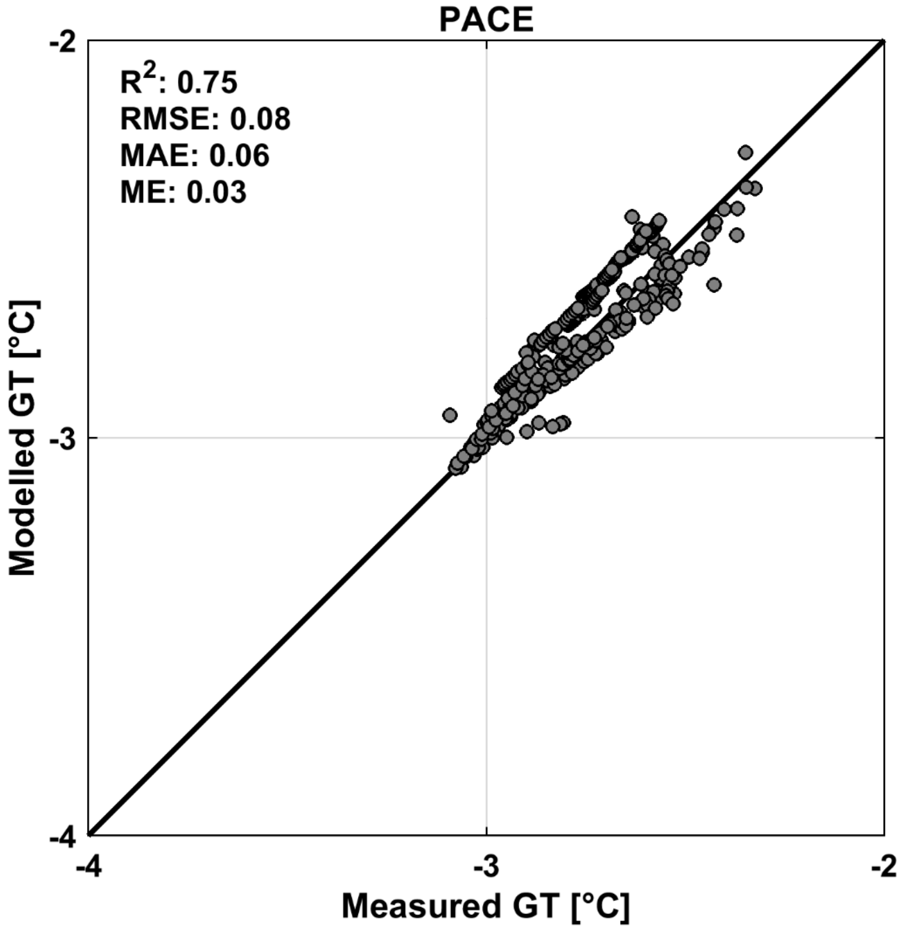

Supplementary Figure S24. Comparison of annual modelled ground temperature (GT) at depths between 5 and 100 m along the Galdhøe profile to ground temperatures measured in PACE borehole in the Jotunheimen Mountains. RMSE-root mean square error, MAE-mean absolute error, ME-mean error. Refer to Figure 1 in the main text for the borehole location.

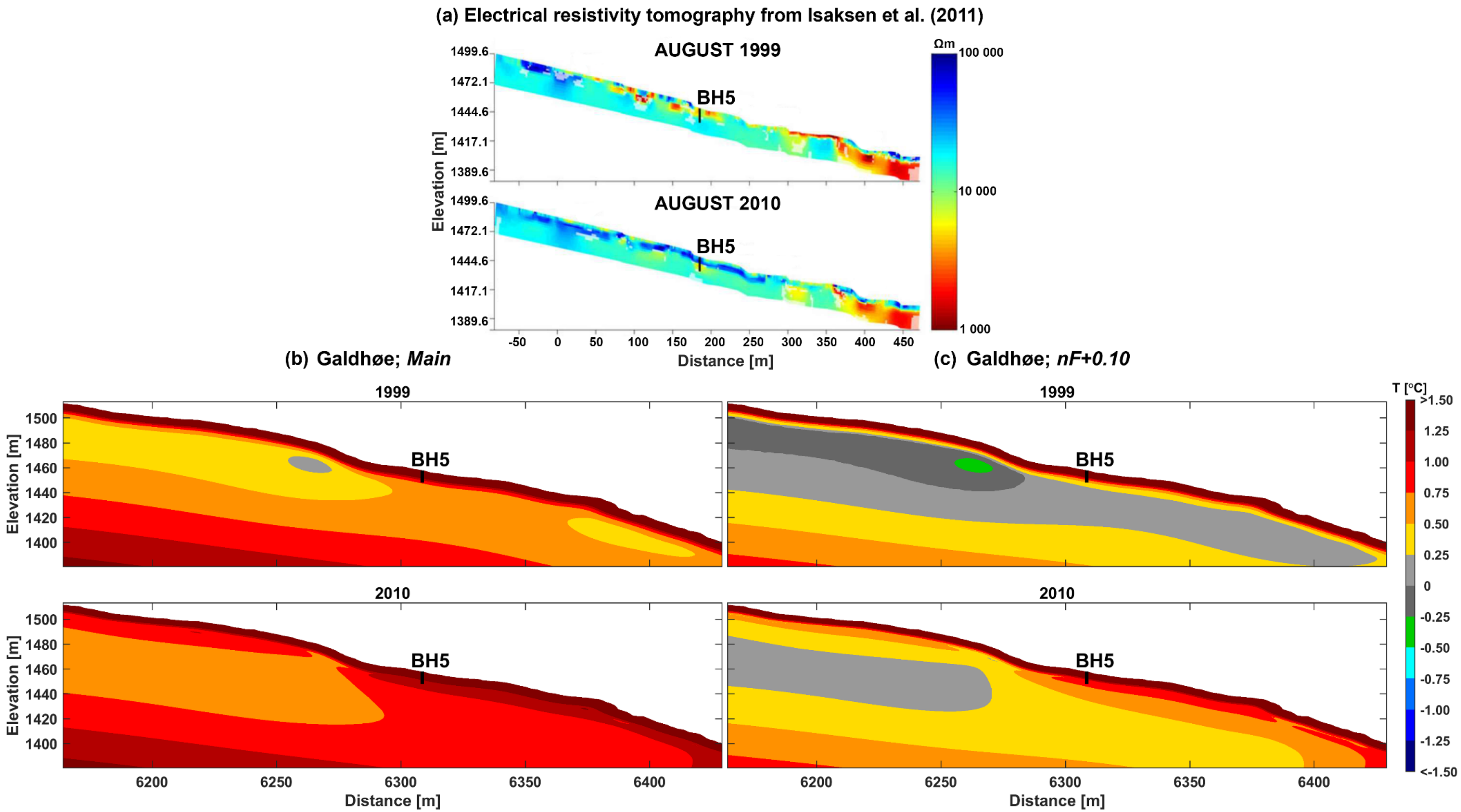

Supplementary Figure S25. Comparison of modelled maximum annual ground temperature along the Galdhøe profile (subplots (b) and (c)) to electrical resistivity tomography (ERT) profiles modified from Isaksen et al. (2011) shown in subplots (a) for years 1999 and 2010. Main simulation is shown in subplots (b) and "nF+0.1" simulation is shown in subplots (c).

Supplementary Tables

Supplementary Table S1. Assumed depths of subsurface layers, along with volumetric fractions of the soil constituents for each layer: θ_w – volumetric water content; θ_m – volumetric mineral content; θ_o – volumetric content of organic matter; θ_a – volumetric air content; z – depth. All sediment classes are underlain by bedrock with the same ground composition as bedrock class (“a”).

z [m]	θ_w [-]	θ_m [-]	θ_o [-]	θ_a [-]
“a”: Bedrock (NGU code 130)				
>0.0	0.05	0.95	0.00	0.00
“b”: Thin till (NGU code 12); “c”: Thin colluvium (NGU code 82)				
0.0–1.0	0.30	0.60	0.00	0.10
“d”: Medium thick till				
0.0–1.0	0.30	0.60	0.00	0.10
1.0–2.0	0.40	0.60	0.00	0.00
“e”: Thick till (NGU code 11); “f”: Thick colluvium (NGU code 81)				
0.0–2.0	0.30	0.60	0.00	0.10
2.0–10.0	0.40	0.60	0.00	0.00
“g”: Weathered material				
0.0–2.0	0.10	0.60	0.00	0.30
“h”: Thin organic cover over bedrock or shallow regolith (NGU code 100)				
0.0–0.5	0.40	0.50	0.10	0.00
“i”: Thin regolith (NGU code 72)				
0.0–1.0	0.10	0.60	0.00	0.30
1.0–2.0	0.40	0.60	0.00	0.00
“j”: Medium thick regolith				
0.0–1.0	0.20	0.60	0.00	0.20
1.0–4.0	0.40	0.60	0.00	0.00
“k”: Fluvial/Alluvial sediments (NGU code 50)				
0.0–1.0	0.10	0.60	0.00	0.30
1.0–10.0	0.40	0.60	0.00	0.00
“l”: Blockfields (NGU code 73)				
0.0–2.0	0.10	0.60	0.00	0.30
2.0–5.0	0.40	0.60	0.00	0.00
“m”: Rock glacier (NGU code 88)				
0.0–2.0	0.05	0.60	0.00	0.35
2.0–5.0	0.10	0.60	0.00	0.30
5.0–35.0	0.40	0.60	0.00	0.00
“n”: Scree				
0.0–5.0	0.02	0.40	0.00	0.58
5.0–various depths	0.60	0.40	0.00	0.00
“o”: Fractured bedrock				
0.0–10.0	0.05	0.80	0.00	0.15
10.0–various depths	0.10	0.90	0.00	0.00
“p”: Heavily fractured bedrock				
0.0–10.0	0.05	0.75	0.00	0.20
10.0–various depths	0.15	0.80	0.00	0.05
“q”: Very thick colluvium				
0.0–2.0	0.05	0.60	0.00	0.35
2.0–5.0	0.10	0.60	0.00	0.30
5.0–30.0	0.40	0.60	0.00	0.00

Supplementary Table S2. Thermal conductivity for the mineral fraction.

Mountain, municipality	**Thermal conductivity [W m^{-1} K^{-1}]**
Mannen, Rauma	2.5
Hogrenningsnibba, Stryn	2.3
Kvernhusfjellet, Stryn	2.3
Ramnanosi, Aurland	3.1
Veslpiggen, Lom	2.7
Galdhøe, Lom	2.7
Gámanjunni 3, Kåfjord	2.9
Ádjit, Storfjord	2.9
Rombakstøtta, Narvik	2.9

Supplementary Table S3. Surface air temperature records used to construct forcing along profiles.

Mountain, municipality	**Meteorological station at the lower elevation along the profile (elevation; years with records)**	**Meteorological station on the mountain plateau (elevation; years with records)**	**Meteorological station(s) with the long-term temperature records (elevation; years with records)**
Western Norway			
Mannen, Rauma	Marstein (67 m; 2010–present)	Mannen (1294 m; 2010–present)	Bergen-Lungegårdshospitalet (17 m; 1861–1895); Bergen-Pleiestiftelsen (22 m; 1895–1926)
Hogrenningsnibba, Stryn	seNorge (200 m; 1957–present)	seNorge (1600 m; 1957–present)	
Kvernhusfjellet, Stryn			
Ramnanosi, Aurland	seNorge (40 m; 1957–present)	Klevavatnet (960 m; 2014–present)	
Jotunheimen			
Veslpiggen, Lom	Juvvasshøe (1894 m; 1999–present)	seNorge (2230 m; 1957–present)	Dombås II (643 m; 1864–1972)
Galdhøe, Lom			
Northern Norway			
Gámanjunni 3, Kåfjord	seNorge (250 m; 1957–present)	Gámanjunni (1237 m; 2016–present)	Tromsø I (38 m; 1872–1926)
Ádjit, Storfjord	Skibotn II (20 m; 2004–present)		
Rombakstøtta, Narvik	Straumsnes (200 m; 2011–present)	Narvik-Fagernesfjellet (1000 m; 2014–present)	

Supplementary Table S4. Logger data. Mean ground surface temperature (GST) is computed as a mean value for the mentioned periods.

Logger site and aspect	Mean GST [°C]	Period	Elevation [m]
Ádjit N	-1.80	Aug 2015–Sep 2020	1230
Ádjit Sh (higher)	0.01	Aug 2015–Sep 2020	1245
Gámanjunni N	-1.31	Aug 2015–Sep 2020	1243
Gámanjunni S	-0.08	Aug 2015–Sep 2020	1220
Gámanjunni W	-1.62	Aug 2015–Sep 2020	1183
Jotunheimen Eh (higher)	-1.78	Sep 2010–Jul 2020	2320
Jotunheimen El (lower)	-2.15	Sep 2010–Jul 2020	2204
Jotunheimen S	-2.23	Sep 2010–Jul 2020	2226
Jotunheimen W	-3.55	Sep 2010–Sep 2018	2179
Loen N	-1.77	Aug 2015–Aug 2018	1709
Loen S	1.40	Aug 2015–Aug 2018	1648
Loen W	1.76	Aug 2015–Aug 2018	1662
Mannen E	2.54	Aug 2015–Jul 2020	1290
Mannen N	1.26	Aug 2015-Jul 2018	1290
Ramnanosi N	0.02	Aug 2016–Jul 2020	1370
Ramnanosi S	2.87	Aug 2016–Jul 2020	1370
Ramnanosi W	1.55	Aug 2016–Jul 2020	1370
Rombakstøtta E	0.10	Aug 2016–Sep 2020	1228
Rombakstøtta N	-0.71	Aug 2016–Sep 2020	1224
Rombakstøtta W	-0.96	Aug 2016–Sep 2020	1208

Supplementary Table S5. Comparison of simulated ground temperatures at the Galdhøe profile and measured ground temperatures in the Jotunheimen Mountains over the 2010s. Refer to Figure 1 in the main manuscript for the borehole locations.

Borehole ID	**Elevation [m]**	**Measured temperature at 10 m depth [°C]**	**Modelled temperature at 10 m depth [°C] in the various simulations**			**Smallest difference**	**Largest difference**
			Main	***nF-0.1***	***nF+0.1***		
PACE	1894	-2.64	-2.44	-1.97	-2.94	0.20	0.67
BH1	1851	-1.92	-2.30	-1.83	-2.75	0.09	0.83
BH2	1771	-1.29	-1.74	-1.31	-2.16	0.02	0.87
BH3	1561	-0.45	0.42	0.80	0.02	0.47	1.25
BH4	1559	-0.51	0.42	0.79	0.00	0.51	1.30
BH5	1458	1.05	0.97	1.33	0.62	0.08	0.43